

Knowledge Aided SAR Processing and GMTI Extensions

Majid Nayeri, Jim Gleason, and David Rieken

8 April, 2004

- **PROPOSED ACTIVITIES and SECOND YEAR RESULTS**
 - Knowledge-Aided Radar Moving Target Focusing
 - Knowledge-Aided SAR Tree-Smear Reduction
 - Knowledge-Aided Clutter Covariance Estimation for GMTI

- **PLANS**
 - Continue Knowledge-Aided Clutter Covariance Estimation

- **Problem:** In SAR, a moving target signature may be spread and displaced in azimuth. The target detection and target (source) location estimation are very challenging due to reduced TCR and the unknown displacement of target signature, respectively. Focusing (compression) of the target signature (for ID) without the knowledge of the target motion over the aperture may be very poor.
- **Solution:** Use the knowledge of the road network on which the moving target is hypothesized to be moving. This knowledge lets the motion induced phase distortion to be estimated.
- **Knowledge Source:**
Fairly accurate Road Network Information is needed.

GD-AIS

- Identified imagery with movers, and with available maps of the roads
- Detected movers hypothesized to move at a **constant speed** on the **known roads**
- Used the knowledge of the road to focus the signatures
- Made comparisons with the existing algorithms to assess performance

- Knowledge-aided processing is employed to focus moving target smears in
 - Select real SAR data
 - Simple synthetic SAR imagery
- There are several algorithms to focus moving targets without any *a priori* information such as **Keystone Remapping** and **Advanced ISAR**.
- Here, **Keystone Remapping** is the algorithm implemented for comparison with the knowledge-aided focusing.
- However, Operational differences between KASSPER processing, **Keystone Remapping**, and **Advanced ISAR** are highlighted.
- Knowledge-aided processing is shown not to suffer from the scaling problem that **Keystone mapping** does. This is particularly important for **ATR**.

- MITRE Corp. developed an algorithm to image moving targets in SAR using Keystone Remapping.
- Keystone Remapping is a processing Kernel that provides the ability to image targets with large range migration over the coherent integration time.
- Consider a SAR system that transmits a series of pulses

$$v(t) = p(t - kT_1) e^{-i2\pi f_c(t - kT_1)}$$

where typically $p(t)$ is the chirp

$$p(t) = e^{-i\frac{\pi B t^2}{T_0}} \text{rect}\left(\frac{t}{T_0}\right)$$

- The received signal from N scatterers after down conversion is

$$s(t', t_k) = \sum_{n=1}^N A_n p\left(t' - \frac{R_n(t_k)}{c}\right) e^{i\frac{4\pi f_c}{c} R_n(t_k)}$$

with Fourier

$$s(f, t_k) = P(f) \sum_{n=1}^N A_n e^{i\frac{4\pi}{c}(f + f_c) R_n(t_k)}$$

where $t' = (t - kT_1)$ is the fast-time, $t_k = kT_1$ is the slow-time, and above is the Fourier Transform in the fast-time.

- The range $R_n(t_k)$ to scatterer n can be expanded in Taylor series about $t_k = 0$ and substituted in the previous relationship to give

$$S(f, t_k) = P(f) \sum_{n=1}^N A_n e^{i \frac{4\pi}{c} (f + f_c) [r_n + \dot{r}_n t_k + \varphi_n(t_k)]}$$

where $\varphi_n(t_k)$ contains quadratic and higher order terms.

Algorithm steps to focus moving targets

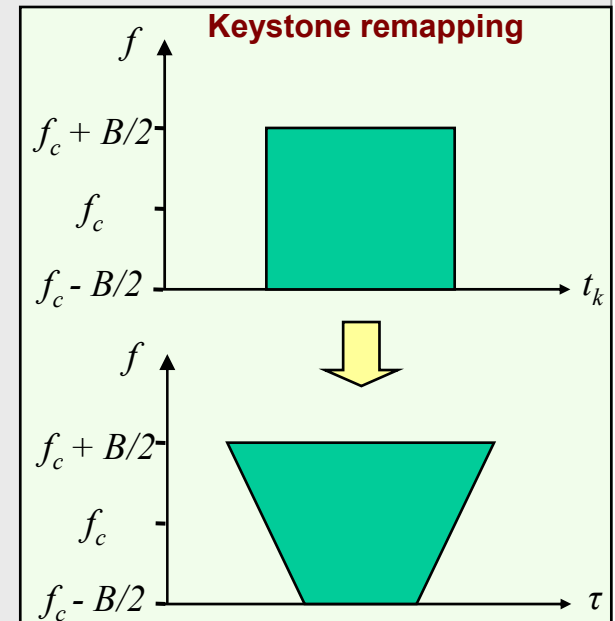
- The linear range migration of scatterers is represented by the coupling term

$$M_n(f, t_k) = e^{i \frac{4\pi}{c} (f + f_c) \dot{r}_n t_k}$$

which may be removed if the time axis is rescaled by

$$t_k = \frac{f_c}{f + f_c} \tau$$

- The residual quadratic range migration errors is removed.
 - Modified or average Dominant scattering methods
- Then, the higher order defocusing terms are removed.
 - Phase gradient method



Fact: Moving targets appear as displaced azimuthal smears in SAR imagery.

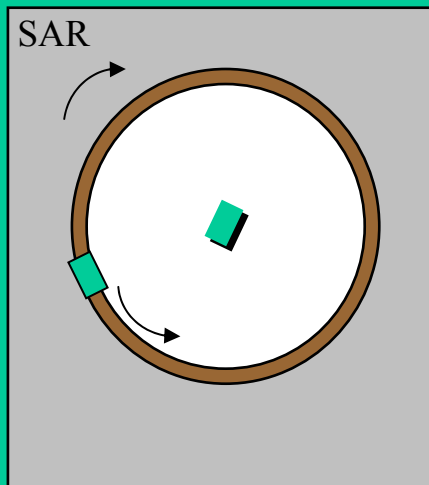
Fact: Present algorithms, *e.g. Keystone Mapping*, focus target smears with incorrect scaling.

Consider an experiment with a set of collected SAR imagery containing two targets:

- a target moving around a circular road
- a stationary target in the center

Details

Diagram of Experiment



- X-band SAR.
- 17.1875° grazing angle.
- Slant range = 26500 ft.
- Altitude = 3700 ft.
- 200 m diameter dirt track.
- Stationary BTR-80 at center.
- M2 going CCW at 12 kph.

SAR image



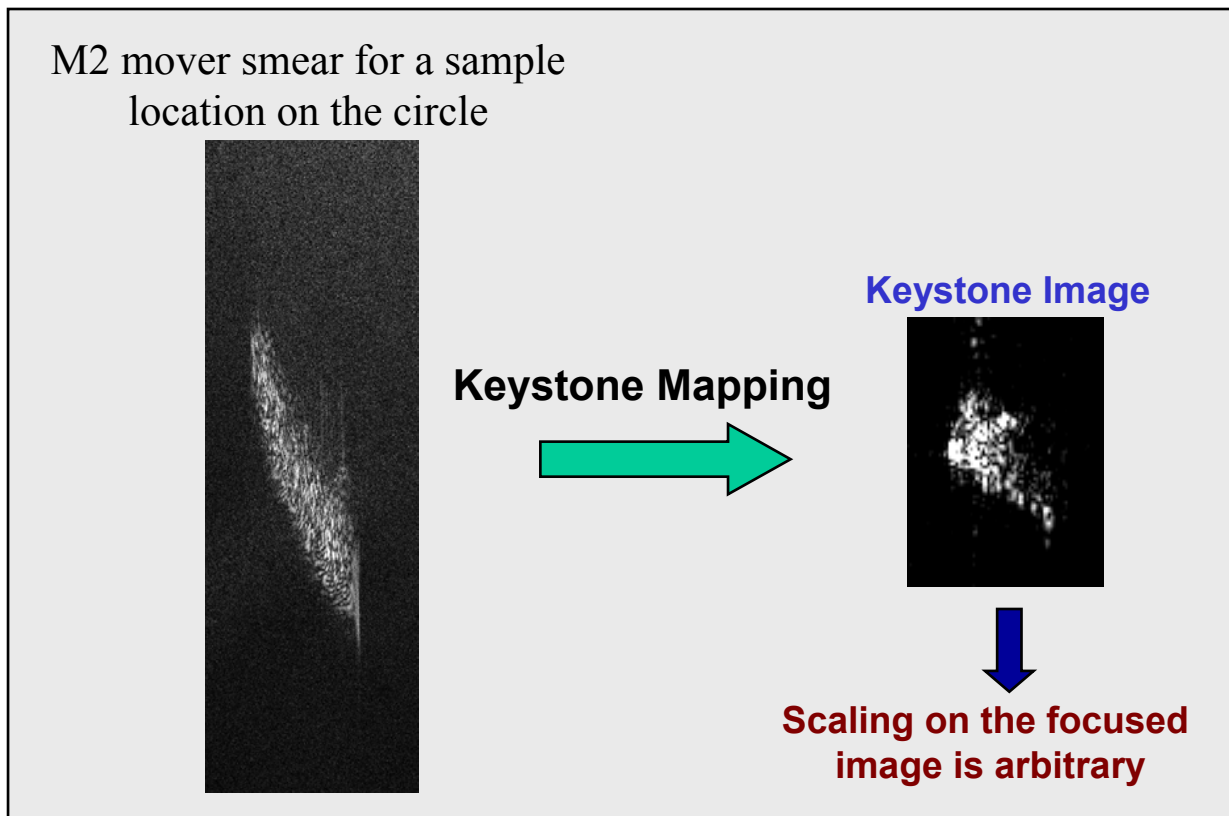
- Range (horiz.)
- Azimuth (vert.)
- 1-ft resolution

Video of moving M2 tank

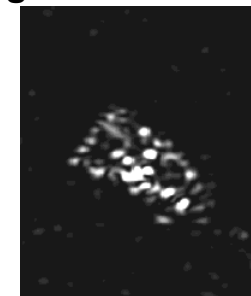


- M2 has translational and rotational motion.
- M2 aspect and elevation angles to radar were recorded at a 4 Hz rate in the aux data.

- ❑ 17 locations around the circular path were examined. We chose one location on the circle with best focusing. (We conjecture that this case is one without smear effects due to out-of-plane, un-modeled, rotational motion.)
- ❑ **The focused image is in the range-Doppler domain and needs to be properly scaled.**
- ❑ Correct scaling is not possible unless the total rotation of the target over the entire coherent integration time is known as well.

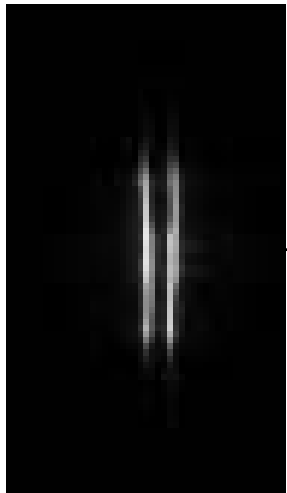


Reference
Image of Stationary M2

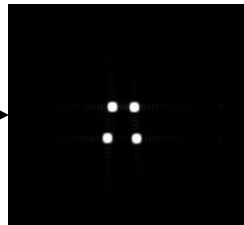


- A set of synthetic SAR images was generated with 4 point targets moving on a circle.
- The point targets were in a trapezoidal arrangement.
- Focusing of the resulting smears was exercised by the Keystone mapping.
- **The resulting imagery have incorrect azimuthal scaling.**

Original Smear of 4 point
Targets moving on a circle
at constant speed



**Focused image obtained
by Keystone remapping
(No information about
the road was used)**



**Comparison between the true relative distances and the
focused relative distances of the 4 point targets**

	Truth	
	<i>Ground Plane</i>	<i>Slant Plane</i>
Top	6.56 ft. (2m)	4.64 ft.
Sides	13.12 ft. (4m)	9.28 ft.
Bottom	8.53 ft. (2.6m)	6.03 ft.
	Measured	
	Keystone	
Top	4.24 ft.	
Sides	5.73, 5.67 ft.	
Bottom	5.48 ft.	



**Keystone yields incorrect
scaling in azimuth.**

Now that there is an azimuthal scaling error with the Keystone Remapping Algorithm, a critical question is raised:

Question: *How well does **a priori knowledge of roads** improve focusing of moving targets, and does the focused imagery have the correct scaling?*

Answer: **The focusing operation should improve (at-least theoretically) and the focused imagery would be in range-azimuth domain (i.e., with correct scaling).**

- Knowledge-aided focusing algorithm uses the **road information** to estimate the slow-time rotation of the rigid-body (target) over the aperture.
- This estimation is performed in step 5 (see below) after some preliminary operations to chip out the smear and remove the translational motion (steps 1-4).
- **This results in an ISAR-like setup, but with time-varying angular velocity.**

Kassper-specific
operations



- **Knowledge-aided processing to focus mover smear**
 1. Generate motion compensated phase history
 2. Apply clutter reduction filter.
 3. Chip out smear.
 4. **Estimate and remove bulk translational motion of the mover.**
 5. Estimate azimuth angle aspect to mover (in the slant plane) by using known sensor motion and known road information and estimated mover direction and motion.
 6. Apply polar-to-rectangular formatting.
 7. Form image with 2D-FFT.

- With the removal of the translational motion, a coordinate system can be chosen at each pulse, such that the radar appears fixed, and the aspect angle of the sensor to the target is known. This is equivalent to ISAR imaging, where the target is moving at an angular velocity $\omega(t)$ about an axis z perpendicular to the line of sight of the radar (see figure).

- We may write

$$r_i = \sqrt{d_i^2 + r_a^2 + 2r_a d_i \sin(\theta_i(t))}$$

$$\cong r_a + d \sin(\theta(t)) \quad , \quad \theta_i(t) = \int_0^t \omega(t') dt' + \theta_i^0$$

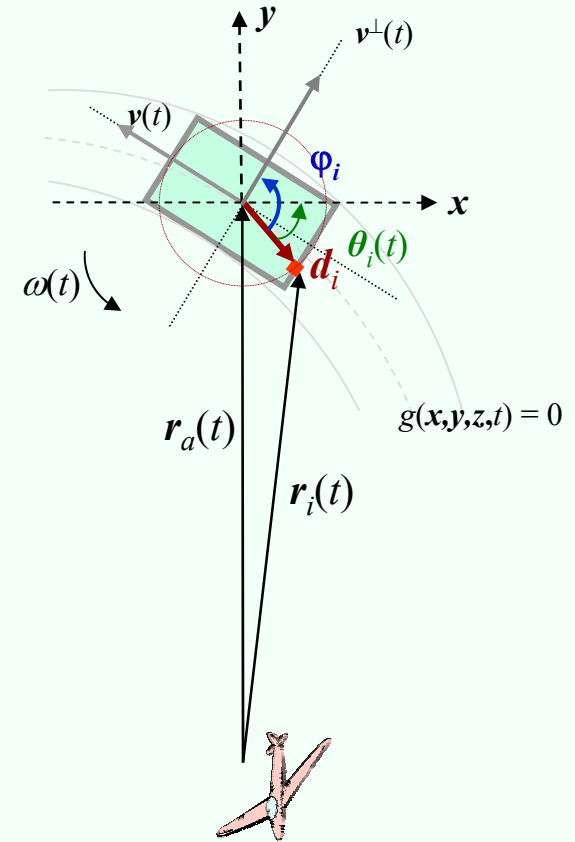
where if we represent the road knowledge by $g(x,y,z,t)=0$, then

$$\theta_i(t) = \varphi_i - \frac{\langle \mathbf{v}^\perp, \mathbf{u}_x \rangle}{\|\mathbf{v}^\perp\|} \quad , \quad \mathbf{u}_x = [1 \ 0]^T$$

$$= \varphi_i - \frac{\langle \nabla \mathbf{g}, \mathbf{u}_x \rangle}{\|\nabla \mathbf{g}\|}$$

- The Doppler frequency is found to be

$$(f_d)_i = \frac{2}{\lambda} \dot{r}_i = \frac{2\dot{r}_a}{\lambda} + \frac{2d}{\lambda} \omega(t) \cos(\theta(t))$$



- $r_a(t)$ = range from radar to center of target
- $r_i(t)$ = range from radar to i th scattering point on target
- d_i = fixed distance from center to i th scattering point on target
- $\theta_i(t)$ = angular distance of the i th scattering center to x
- $\mathbf{v}(t)$ = velocity vector (target axis in the direction of motion)
- φ_i = fixed angle from the i th scattering center to $\mathbf{v}^\perp(t)$

- The received signal model after dechirp is

$$s(t_n, \hat{t}) = \text{rect}\left(\frac{\hat{t} - 2r_a/c}{T_p}\right) e^{-j\frac{4\pi\gamma}{c}\left(\hat{t} + \frac{f_c}{\gamma} - \frac{2r_a}{c}\right)(r-r_a)}$$

Where t_n is slow time, \hat{t} is fast time, f_c is center frequency, γ is chirp rate, T_p is pulse length, and r is a function of t_n .

- The polar format radius is:

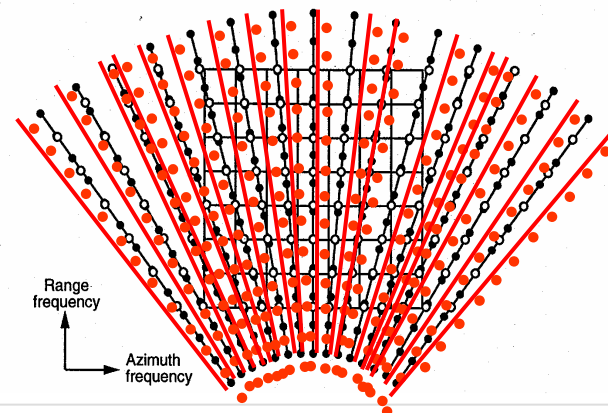
$$K_p(t_n, \hat{t}) = \frac{4\pi\gamma}{c}\left(\hat{t} + \frac{f_c}{\gamma} - \frac{2r_a}{c}\right)$$

- The polar angle is $\omega(t_n)$.
- After polar format transformation, the phase history becomes:

$$\begin{aligned} \Phi(t_n, \hat{t}) &= K_p[x_0 \sin(\omega(t_n)) + y_0 \cos(\omega(t_n))] \\ &= K_a x_0 + K_r y_0 \end{aligned}$$

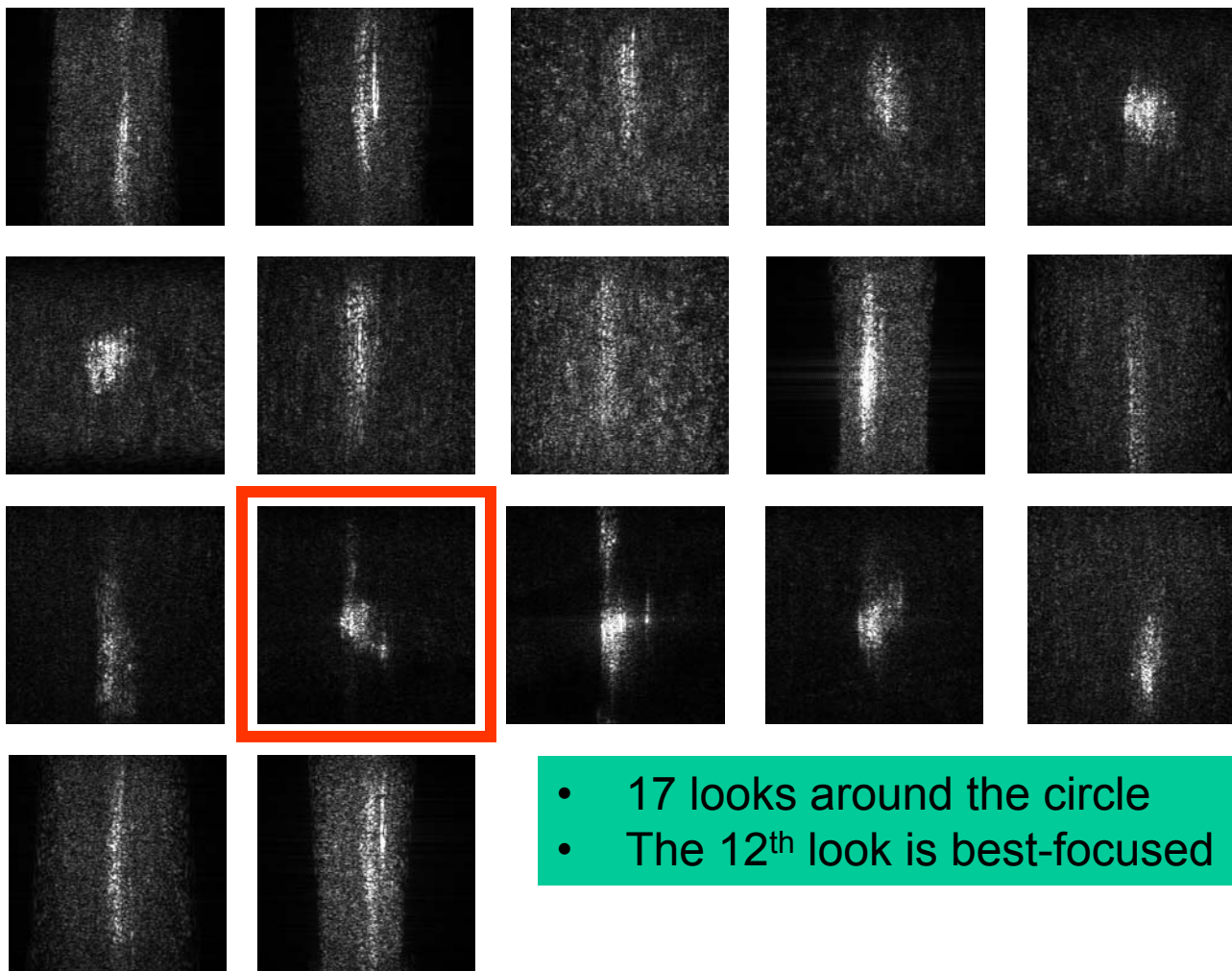
- Where K_a is the spatial sampling distance in azimuth, and K_r is the spatial sampling distance in range.

- The polar grid shows black dots where samples would be collected if $\omega(t_n)$ the aspect angle, is linearly changing with pulse time.
- The clear dots show evenly-spaced interpolated points in range, which is the first step in generating a rectangular grid of points.
- The red lines show a case where $\omega(t_n)$ is not a linear function of pulse time.
- It is still desirable to interpolate to the same clear dots as before, however, the input red samples must not violate Nyquist sampling (or else the output image resolution will be reduced).
- In fact, for 1 foot resolution at X-band, there must be ~ 3 degrees of angle, and the number of range and azimuth samples in the inscribed rectangular output grid are given by: $n_{phr} = K_r/\rho_r$, and $n_{pha} = K_a/\rho_a$. Too large a space between samples can affect the choice of the interpolation scheme and the sensitivity of the interpolation result to noise.



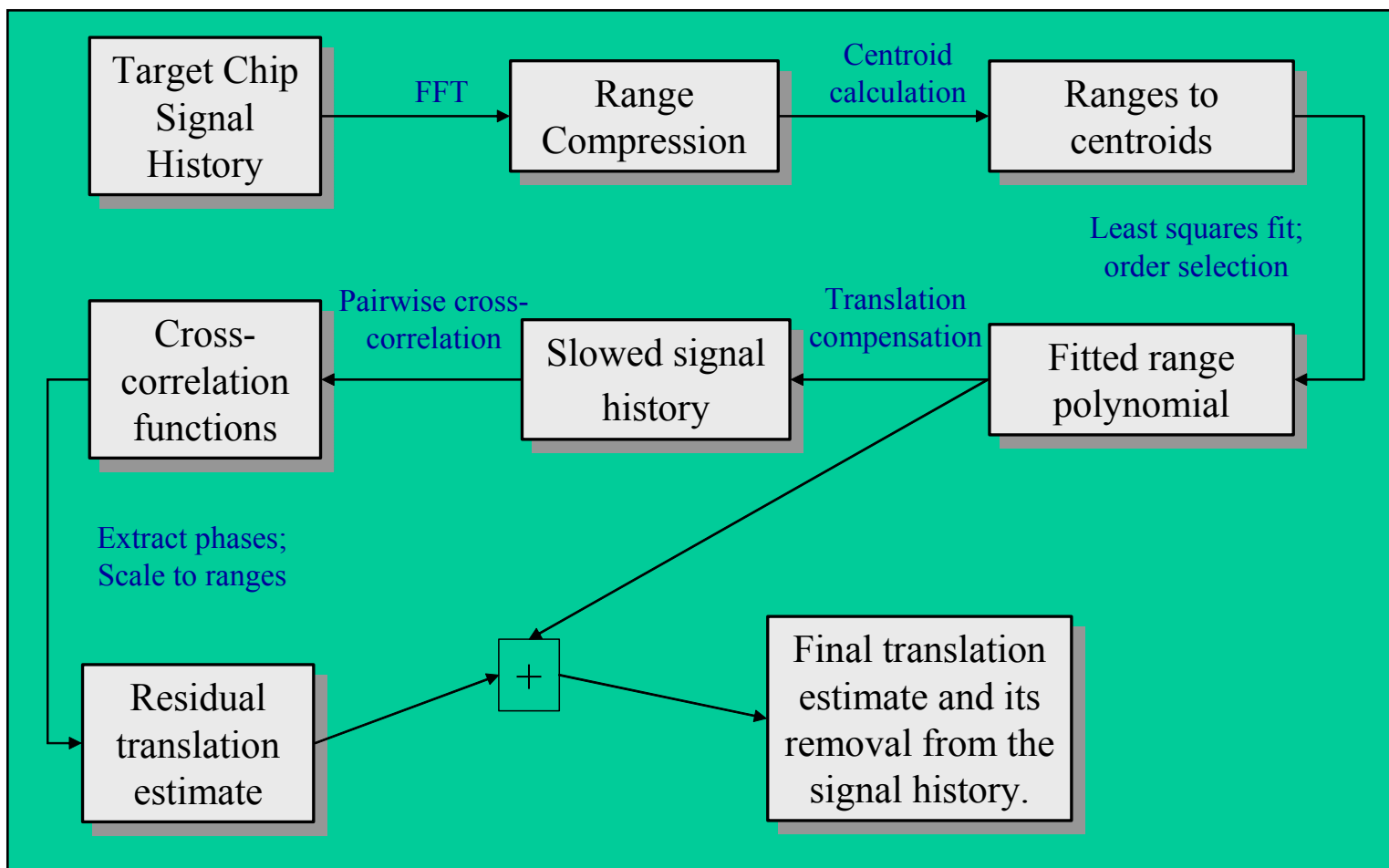
Unevenly-spaced $\theta(t_n)$ polar format data along red lines.

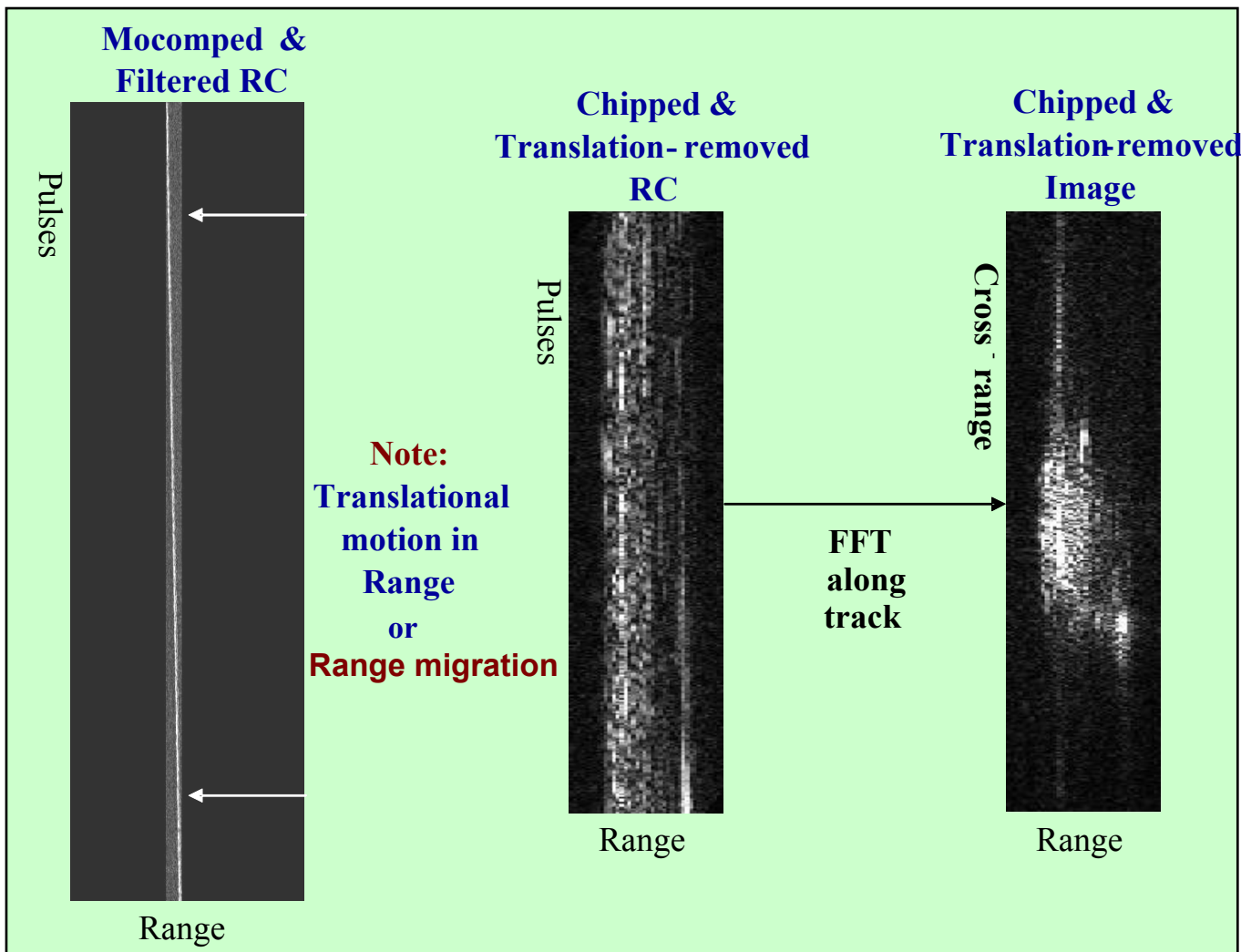
For this experiment, the knowledge is the geo-coordinates of the circular road



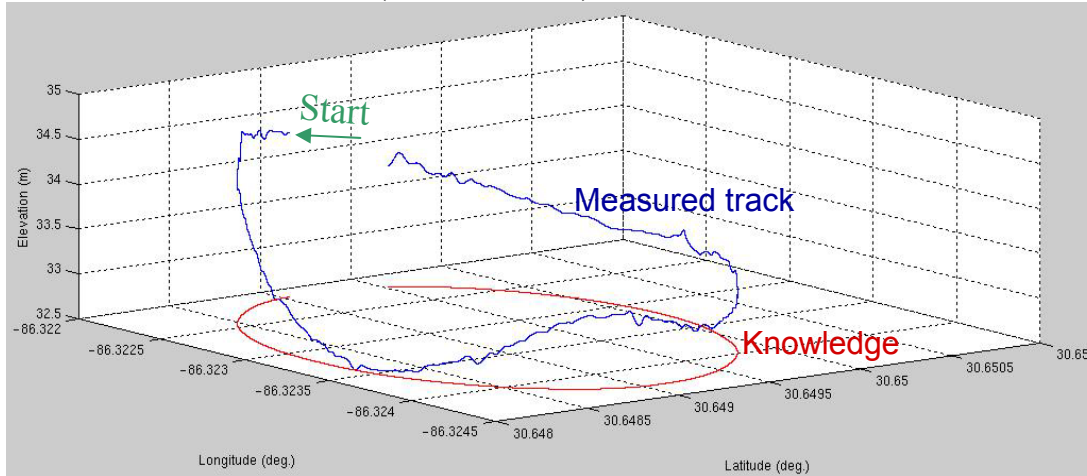
- 17 looks around the circle
- The 12th look is best-focused

Estimation and removal of bulk translational motion effects





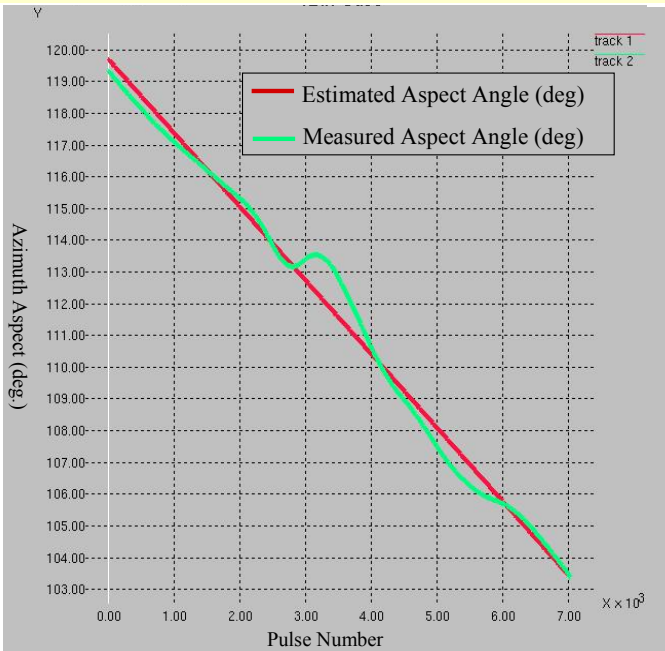
(Lat, Lon, Alt) of M2 Mover



With translational motion removed

- Estimate the aspect angle by using the road knowledge
- Interpolate the resulting polar VPH onto a rectangular grid
- Take 2-d FFT

The azimuth angle is determined from the SAR sensor position and the target direction and position on the 'road' (in red above).



Chipped & Translation-removed Image

Image with polar-to-rectangular formatting and 2-d FFT (grazing angle = 17.1875°).

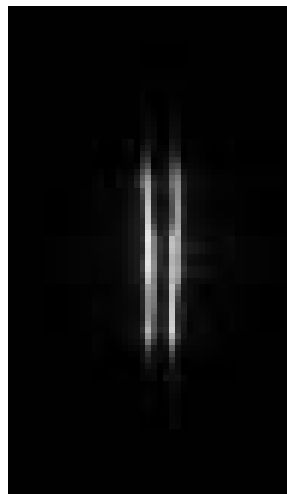
Double Click on the movie of a stationary M2 at scene center with the sensor in a circular flight around it (~300 degrees of look direction in the movie). (grazing angle = 16.99°)

Cross-range

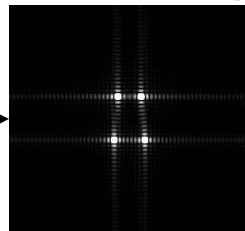
Range

- A set of synthetic SAR images was generated with 4 point targets moving on a circle.
- The point targets were in a trapezoidal arrangement.
- Focusing of the resulting smears was exercised by Knowledge-aided focusing.
- **No azimuthal scaling discrepancy is observed with this method.**

Original Smear of 4 point
Targets moving on a circle
at constant speed



Focused image obtained
by Road-Knowledge-
aided focusing



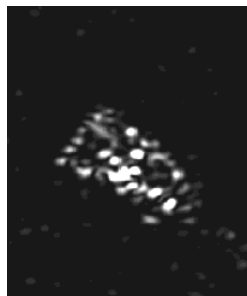
Comparison between the true relative distances and the
focused relative distances of the 4 point targets

Truth		
	<i>Ground Plane</i>	<i>Slant Plane</i>
Top	6.56 ft. (2m)	4.64 ft.
Sides	13.12 ft. (4m)	9.28 ft.
Bottom	8.53 ft. (2.6m)	6.03 ft.
Measured		
Knowledge-aided		
Top		4.75 ft.
Sides		9.75 ft.
Bottom		6.5 ft.

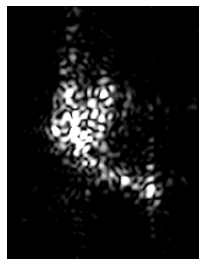


**Correct scaling in azimuth
is achieved.**

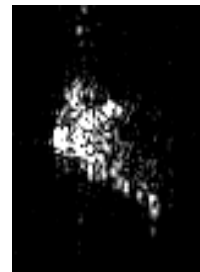
Stationary Image of M2 (case 12)



Knowledge-aided Image



Keystone Image



- The Keystone image looks a bit sharper for this exercise.

The **red** and **blue** colors highlight the differences in the algorithms.

❑ Keystone Processing

- Generate motion compensated phase history.
- Apply clutter reduction filter. (Might not have been done in original formulation.)
- Chip out smear.
- Apply keystone algorithm which performs a 1D polar-to-partially rectangular formatting.
- Apply autofocus algorithm to resulting rangewalk-corrected smear.
- Form image with 2D-FFT.
- Scaling ambiguity in azimuth



❑ KASSPER Processing

- Generate motion compensated phase history
- Apply clutter reduction filter.
- Chip out smear.
- Estimate and remove bulk translational motion of mover.
- Estimate azimuth angle aspect to mover (in the slant plane) by using known sensor motion and known road information and estimated mover direction and motion.
- Apply polar-to-rectangular formatting.
- Form image with 2D-FFT.
- Iterate over 17 locations around the circular path.
- Choose cases without smear effects due to out-of-plane, un-modeled, rotational motion.
- No scaling ambiguity in azimuth.

❑ Advanced ISAR Processing

- Generate motion compensated phase history
- Clutter background is low, so no need to filter.
- Chip out smear.
- Estimate and remove bulk translational motion of mover using estimated mover motion and correlation pull-in.
- Estimate azimuth angle aspect to mover by using known sensor motion and estimated mover motion.
- Estimate rotational motion with focusing of clusters of point-like scatterers.
- Apply polar-to-rectangular formatting, with out-of-plane data projected to the image plane.
- Form image with 2D-FFT.
- Scaling ambiguity in azimuth.



❑ KASSPER Processing

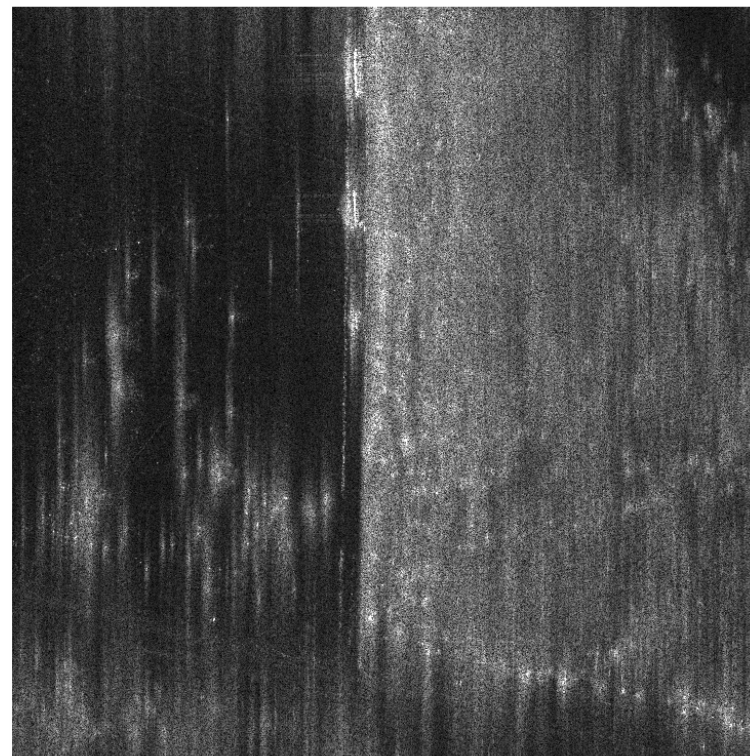
- Generate motion compensated phase history
- Apply clutter reduction filter.
- Chip out smear.
- Estimate and remove bulk translational motion of mover.
- Estimate azimuth angle aspect to mover (in the slant plane) by using known sensor motion and known road information and estimated mover direction and motion.
- Apply polar-to-rectangular formatting.
- Form image with 2D-FFT.
- Iterate over 17 locations around the circular path.
- Choose cases without smear effects due to out-of-plane, un-modeled, rotational motion.
- No scaling ambiguity in azimuth.

- Target smear can be properly **scaled** and **focused** with *a priori* knowledge of the road provided out-of-plane, un-modeled, rotational motion is minimal.
- Chances are improved with multiple looks at the target.
- The azimuth aspect angle must be sufficient for the desired resolution (3 degrees for 1 ft. resolution).
- The *a priori* knowledge can provide the necessary information for correcting the scaling issue with the Keystone Remapping.

- **Problem:** For long enough integration time, the streaks caused by blowing trees may obscure targets in the open and along treelines.
- **Solutions:**
 - Prediction-based filtering using the knowledge of the treed areas
- **Knowledge Source:** DFAD

- **GD-AIS identified single aperture examples with significant effects of moving trees.**
- GD-AIS Extended and applied the prediction-based decomposition by using 1-D and 2-D prediction filters over the open and treed areas identified by DFAD.
- The underlying smear is modeled as an added noise to predictable signals (point targets) in which the noise decorrelates over the aperture.

T2074v201.swab



The underlying smear is modeled as an additive noise, added to predictable signals (point targets), that decorrelate over the aperture. That is, the signal history may be written as

$$X(k, f) = S(k, f) + n(k, f)$$

where

$$\begin{aligned} k &= \text{Pulse Number} \\ f &= \text{Spatial Frequency} \end{aligned}$$

The covariance function of $n(k, f)$ gets arbitrarily close to zero beyond K pulses or beyond F frequencies, i.e.,

$$R_n(\Delta k, \Delta f) < \varepsilon \quad , \quad |\Delta k| \geq K \quad , \quad |\Delta f| \geq F$$

ε = A small positive number

K = A positive integer

F = A positive number

(In typical SAR, uniform clutter is usually assumed to be uncorrelated from pixel-to-pixel, hence frequency-to-frequency. Consequently, $F = 1$.)

1. The 2-D Separable predictor is a two stage algorithm:

○ **First stage: Solve**

$$\min_a E \left| X(k, f) - X^a(k, f) \right|^2$$

where

$$X^a(k, f) = \sum_{i=K+1}^{K+N} a_i X(k-i, f)$$

○ **Second stage: Solve**

$$\min_b E \left| X^{a*}(k, f) - \sum_{j=1}^M b_j X^{a*}(k, f - j f_s) \right|^2$$

where f_s is the spatial frequency sampling interval.

2. The Minimum Variance Method (MVM) maximizes SIR for point targets by solving

$$\min_{A(\mathbf{r})} E \left| A^H(\mathbf{r}) \mathbf{X} \right|^2 \quad s.t. \quad A^H(\mathbf{r}) \mathbf{W}(\mathbf{r}) = 1$$

where \mathbf{r} is the location of a point target, \mathbf{X} is the rasterized vector of the 2-D signal history $X(k, f)$, and \mathbf{W} is the Kronecker product of 1-D Fourier transform vectors.

Identical images

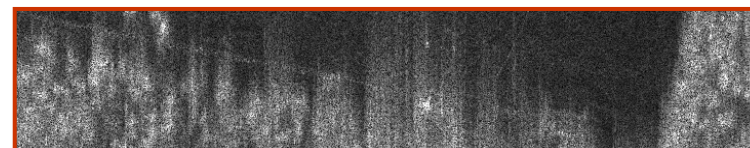
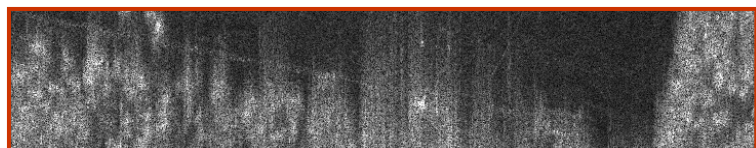
T2067v103.swab



T2067v103.swab



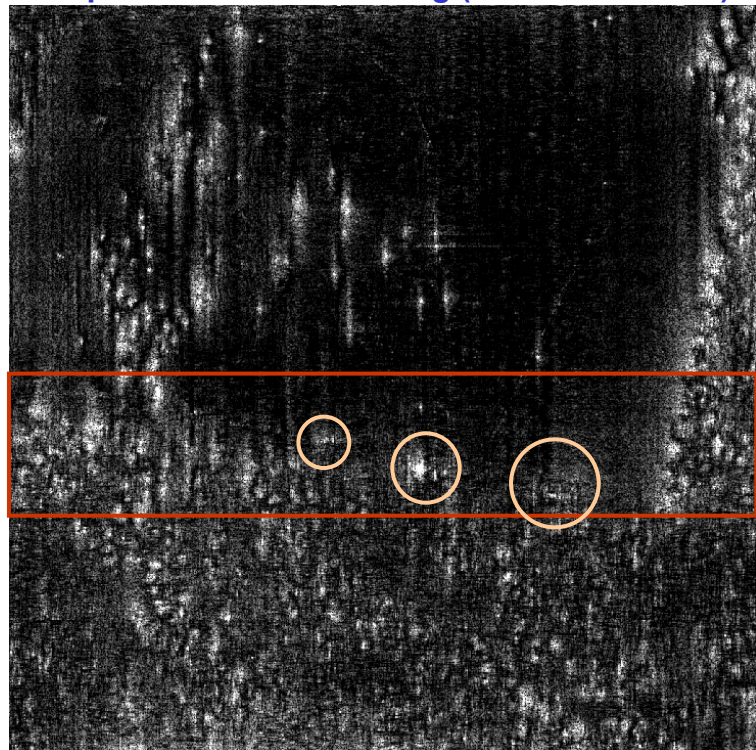
Toggle back and forth between this and the next viewgraph



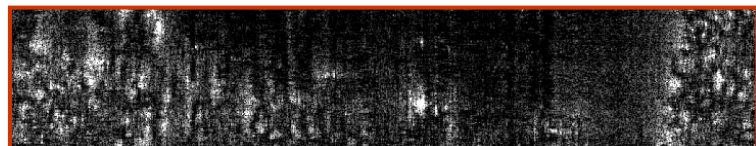
The knowledge of the treeline dictates where and how to process

- Contrary to the point scatterers, tree-smears tend to decorrelate over the aperture.
- Predictive algorithms can restore the predictable (i.e., point scatters) and mitigate the unpredictable (i.e., smears)

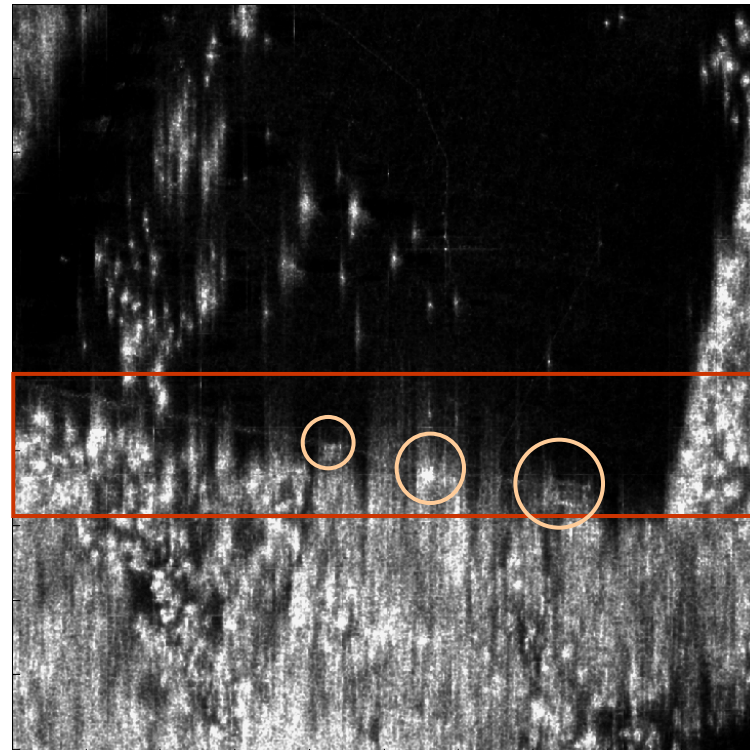
Separable 2-D AR Filtering (64th order model)



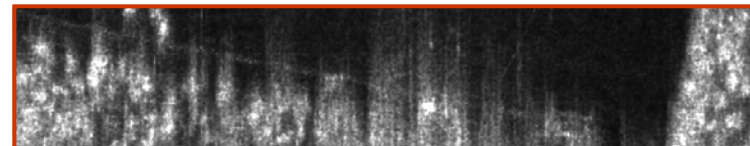
The knowledge of the treeline dictates
where and how to process



Full MVM Image



The knowledge of the treeline dictates
where and how to process



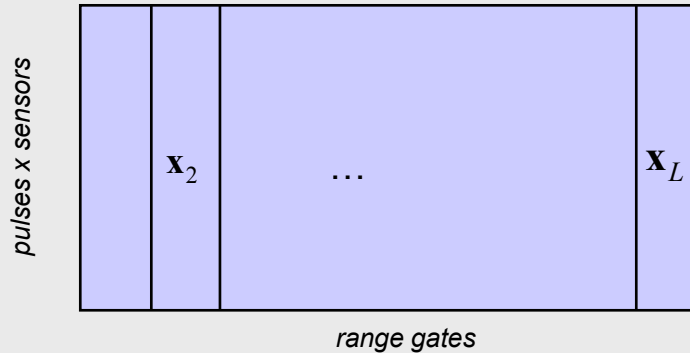
- Two predictive methods were developed to reduce the smear caused by windblown trees.
- The separable 2-D prediction is quite effective in removing the smear while preserving **some** point scattering centers on target.
- The non-separable 2-D prediction (MVM) is quite effective in reducing the background clutter and preserving point-target signatures in the image.
- The DFAD provides the knowledge of the tree-line by which targets may be located and the moving trees smear may affect the most.

- **Problem:** Improve the clutter covariance estimate in STAP MTI
 - clutter is a non-stationary random process
 - proper covariance estimation with a single CPI is an under-determined problem
- **Solution:** Statistically infer the clutter covariance matrix at each range gate from previously collected single/multi-channel SAR/GMTI CPIs
- **Knowledge Source:** Previously collected SAR/GMTI data sets

- GD-AIS has recognized that by with multiple GMTI CPIs available, the problem of non-stationary clutter covariance estimation is not ill-posed as it is with just one CPI. Well-known problems in clutter covariance estimation should be revisited with the new data set. This is the direction in which our effort is focused.

pre-KASSPER signal model

STAP data cube:



STAP covariance estimation is forced to assume i.i.d space-time snapshots:

$$\mathbf{x}_l \sim CN(\mathbf{0}, \mathbf{R}) \quad \forall l$$

so that covariance estimate is:

$$\hat{\mathbf{R}} = \frac{1}{L} \sum_{l=1}^L \mathbf{x}_l \mathbf{x}_l^H$$

KASSPER signal model

current data set : $\mathbf{z} = \mathbf{A}\mathbf{s}$

previous data sets : $\mathbf{z}_n = \mathbf{A}_n \mathbf{s}_n \quad \forall n \in [1, \dots, N]$

$$\mathbf{R} \equiv E[\mathbf{z}\mathbf{z}^H] = \mathbf{A}^H \Sigma^{(i)} \mathbf{A}$$

$$\mathbf{R}_n \equiv E[\mathbf{z}_n \mathbf{z}_n^H] = \mathbf{A}_n^H \Sigma^{(i)} \mathbf{A}_n$$

$\mathbf{s}, \mathbf{s}_1, \dots, \mathbf{s}_N$ are realizations of the clutter reflectivity for each data set.

We model them as i.i.d., $CN(\mathbf{0}, \Sigma)$.

$\mathbf{A}, \mathbf{A}_1, \dots, \mathbf{A}_N$ represent the clutter response in the radar signal (range, Doppler, & DoA)

- We have made two changes to the signal model, which make estimation of the non-stationary clutter covariance possible:
 - A structure is imposed on the covariance matrix
 - More than one snapshot is available
- Either of these constraints imposed separately are difficult to impose. However a maximum-likelihood formulation is possible, although not in a closed form.

Expectation-Maximization iterative estimate:

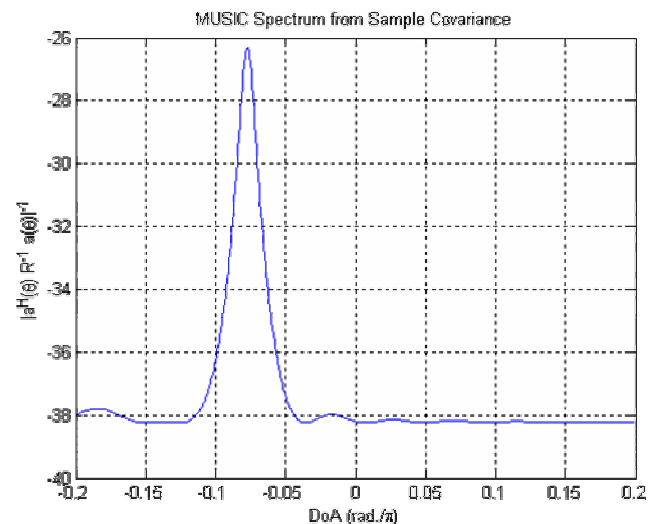
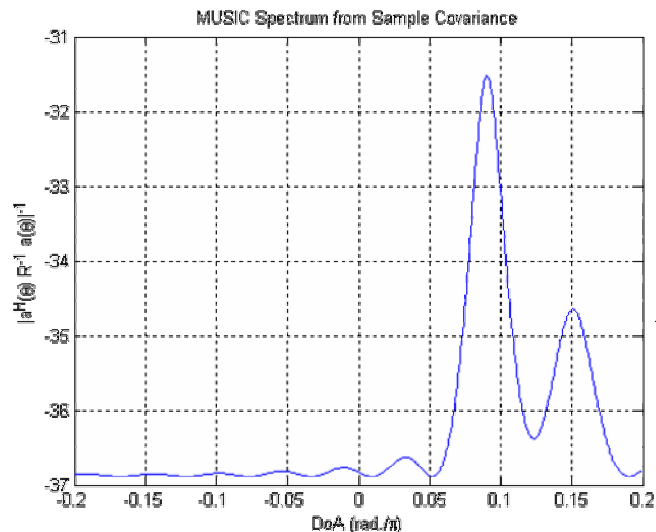
$$\hat{\Sigma}^{(i+1)} = \Sigma^{(i)} + \frac{1}{N+1} \hat{\Sigma}^{(i)} \mathbf{A}^H \left(\left(\hat{\mathbf{R}}^{(i)} \right)^{-1} \mathbf{z} \mathbf{z}^H \left(\hat{\mathbf{R}}^{(i)} \right)^{-1} - \left(\hat{\mathbf{R}}^{(i)} \right)^{-1} \right) \mathbf{A} \hat{\Sigma}^{(i)}$$

$$+ \frac{N}{N+1} \sum_{n=1}^N \hat{\Sigma}^{(i)} \mathbf{A}_n^H \left(\left(\hat{\mathbf{R}}_n^{(i)} \right)^{-1} \mathbf{z}_n \mathbf{z}_n^H \left(\hat{\mathbf{R}}_n^{(i)} \right)^{-1} - \left(\hat{\mathbf{R}}_n^{(i)} \right)^{-1} \right) \mathbf{A}_n \hat{\Sigma}^{(i)}$$

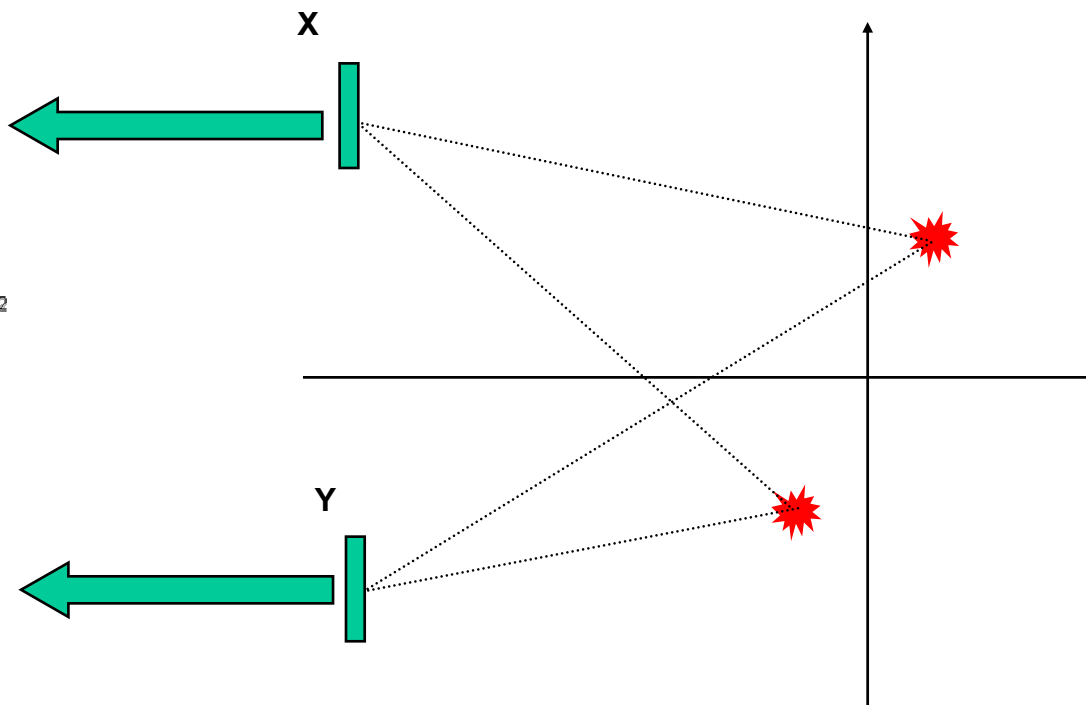
Derive clutter covariance estimate from clutter power using:

$$\hat{\mathbf{R}}^{(i)} = \mathbf{A}^H \hat{\Sigma}^{(i)} \mathbf{A}$$

$$\hat{\mathbf{R}}_n^{(i)} = \mathbf{A}_n^H \hat{\Sigma}^{(i)} \mathbf{A}_n$$

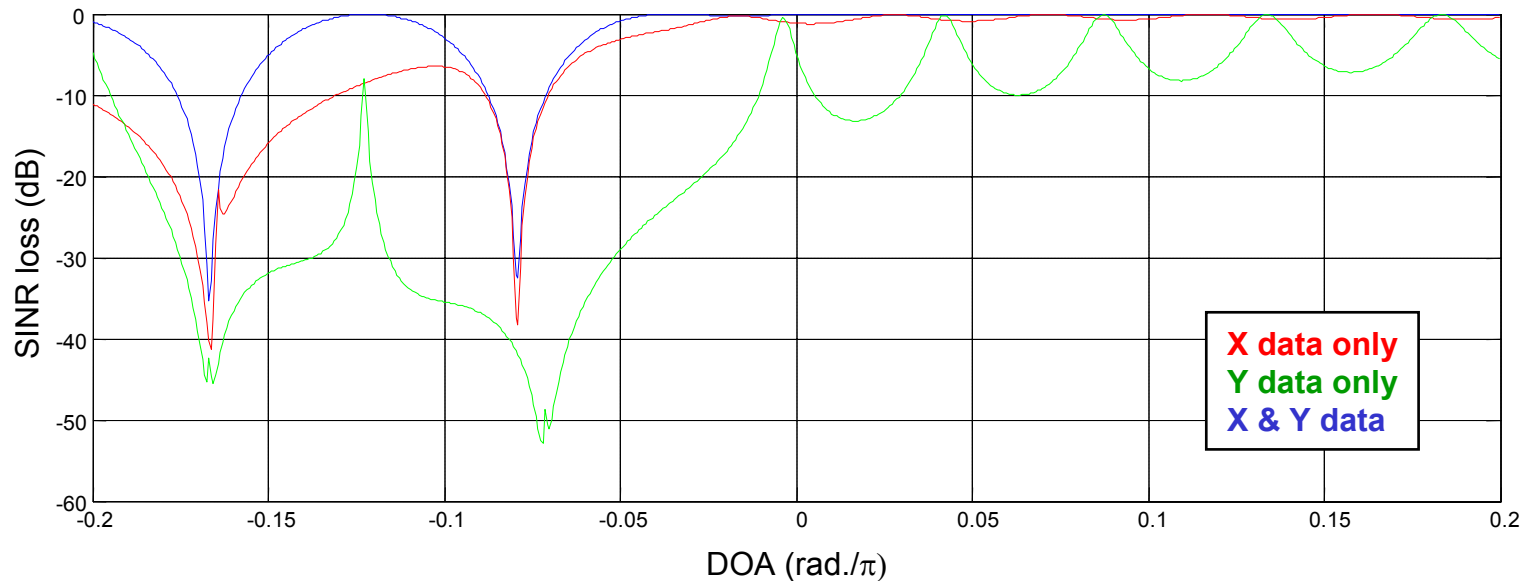


Passive Array Simulation in Matlab

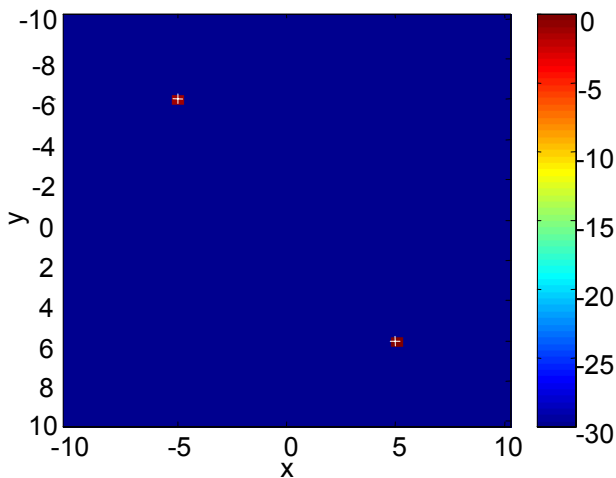
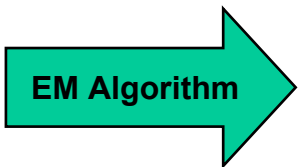


- One snapshot, each, from two 15-element ULAs.
- Two white, uncorrelated signal sources
- MUSIC spectrum computed using diagonally loaded sample covariance matrices

SINR loss for different training sets



signal snapshots



Covariance Estimate

- GD-AIS has considered the possibility of covariance estimation using a Bayesian paradigm

$$p(\mathbf{R} | \mathbf{z}, \mathbf{z}_1, \dots, \mathbf{z}_N) = \frac{p(\mathbf{z} | \mathbf{R})p(\mathbf{R} | \mathbf{z}_1, \dots, \mathbf{z}_N)}{p(\mathbf{z} | \mathbf{z}_1, \dots, \mathbf{z}_N)}$$

- The first term in the numerator is well-known, and it may be possible to compute the distribution by Monte Carlo methods if the second term were known:

$$\begin{aligned} p(\mathbf{R} | \mathbf{z}_1, \dots, \mathbf{z}_N) &= \int d\Sigma p(\mathbf{R}, \Sigma | \mathbf{z}_1, \dots, \mathbf{z}_N) \\ &= \int d\Sigma p(\mathbf{R} | \Sigma, \mathbf{z}_1, \dots, \mathbf{z}_N) p(\Sigma | \mathbf{z}_1, \dots, \mathbf{z}_N) \\ &= \int d\Sigma \frac{p(\mathbf{R} | \Sigma, \mathbf{z}_1, \dots, \mathbf{z}_N) p(\mathbf{z}_1, \dots, \mathbf{z}_N | \Sigma) p(\Sigma)}{p(\mathbf{z}_1, \dots, \mathbf{z}_N)} \end{aligned}$$

- Generating covariance matrices according to this distribution is computationally intensive.
- This method has not produced satisfactory results to date

- Clutter Covariance estimate is computed from clutter map that is formed by considering multiple non-coherent synthetic apertures.
- SAR processing won't work with this signal model, so we use the E-M algorithm.
- Simulations with simple, passive array problems demonstrate the promise of this approach with a measured improvement in SINR loss.
- Bayesian estimators may have potential, but that has yet to be demonstrated



- GD-AIS proposes to support KASSPER by continuing the initiated effort in the GMTI clutter covariance estimation.
- Continue MLE algorithm development:
 - Look for ways to speed it up without sacrificing performance
 - Analyze the effects of movers in training data
 - Analyze the effects of array calibration errors
- Pursue Bayesian estimation possibilities
- Continue testing algorithm on KASSPER Data Set 2, and multichannel DCS data